# **Knee Exoskeleton Reduces Muscle Effort and Improves Balance During Sit-to-Stand Transitions After Stroke: A Case Study**

Sergei V. Sarkisian<sup>1\*</sup>, Andrew J. Gunnell<sup>1\*</sup>, K. Bo Foreman<sup>1,2</sup>, and Tommaso Lenzi<sup>1</sup>, *Member, IEEE* 

Abstract— After a stroke, the weight-bearing asymmetry often forces stroke survivors to compensate with overuse of the unaffected side muscles to stand up. Powered exoskeletons can address this problem by assisting the affected limb during sit-tostand transitions. However, there is currently no experimental evidence demonstrating the efficacy of this intervention with the target population. This study explores controlling a powered knee exoskeleton with EMG signals to assist a stroke patient during sit-to-stand transitions. Our results show decreased peak knee torques by 6.24% and 11.9% on their unaffected and affected sides, respectively, while wearing the exoskeleton. Additionally, the peak value of the EMG signal decreased by 29.3% and 21.9%, and the integrated EMG signal value decreased by 46.7% and 36.1% on their affected vastus medialis and lateralis while wearing the exoskeleton, respectively. Finally, our results indicate improved medial-lateral balance by 61.2%. 81.6%, and 70.0% based on the degree of asymmetry (DOA), the center of pressure (COP), and the center of mass (COM), respectively. These results support the efficacy of using powered exoskeletons for high-torque tasks such as sit-to-stand transitions with stroke survivors.

# I. INTRODUCTION

Stroke is the leading cause of long-term disability in the US [1]. Approximately 80% of stroke survivors experience hemiparesis and muscle weakness resulting in difficulty or inability to move one side of the body. Abnormally low strength and early onset of fatigue, symptoms of hemiparesis severely reduce walking speed, efficiency, and endurance [2][3]. Even with the best rehabilitation therapy, most stroke survivors have permanent impairments that reduce their ability to ambulate [4]. Beyond rehabilitation, these individuals could benefit from the use of assistive technologies that compensate for the weakness of the affected lower limb.

Sit-to-stand transitions are extremely difficult for stroke survivors with chronic hemiparesis. Due to the lack of strength and control in the paretic leg, individuals with hemiparesis compensate by overexerting their unaffected lower limb during sit-to-stand transitions. This strategy promotes an unnatural postural sway and a marked weight-bearing asymmetry between the affected and unaffected leg [5][6], which have been linked to increasing the risk of falls

\*Equal contribution. This work was supported in part by the National Institute for Occupational Safety and Health under Grant T42/CCT810426 and in part by the US Department of Defense under Grant W81XWH-16-1-0701 and in part by the National Science Foundation under Grant 2046287. All authors are currently affiliated with the University of Utah. ¹Authors affiliated with the Department of Mechanical Engineering, Robotics Center. ²Authors affiliated with the Department of Physical Therapy and Athletic Training. (Corresponding author: Sergei V. Sarkisian, email: sergei.sarkisian@utah.edu).

[5] because the majority of work necessary to perform the sitto-stand transition is provided by the unaffected lower limb [7]. In addition, perceived effort and fatigue are much greater in subjects with hemiparesis than in healthy individuals [8]. The reduced ability to perform sit-to-stand transitions has a negative effect on mobility, independence, and quality of life [9].

Powered exoskeletons have been proposed to assist stroke survivors and, more generally, individuals with a physical disability during sit-to-stand transitions. Powered knee exoskeletons are particularly promising to solve this problem because up to 70% of the work necessary to stand up from a seated position is done by the biological knee joint in healthy individuals [10]. Many knee exoskeletons have been developed by research laboratories to explore several design and control issues [11]. After years of development, powered knee exoskeletons have achieved a relatively low weight, high maximum torque, and good torque controllability, satisfying the requirements to assist sit-to-stand transitions [12][13].

Several studies have addressed the feasibility of powered exoskeletons with healthy subjects. The primary outcome for most of these studies is muscle effort, which is assessed using electromyography (EMG). These studies show that reducing the muscle effort with a powered exoskeleton is possible in young, healthy individuals [14]. They also show that the timing of the exoskeleton assistance [15] and the correct detection of the movement initiation [16] are critical for the success of the assistance. Moreover, studies show that the alignment between the powered axis of the knee exoskeleton and the anatomical knee joint axis affects comfort and symmetry during assisted sit-to-stand transitions with healthy subjects [17][13]. However, experiments with individuals with hemiparesis are still missing. Thus, the effect of powered knee exoskeletons in this population is unknown.

In this paper, we assess the effects of an autonomous, unilateral knee exoskeleton on sit-to-stand transitions in one individual with hemiparesis due to stroke. Our hypothesis is that by providing assistive knee torque proportional to the EMG activation of the quadriceps of the affected side, a powered knee exoskeleton will reduce effort and improve symmetry. To test this hypothesis, we asked one individual with hemiparesis to perform sit-to-stand transitions with and without an autonomous, unilateral powered knee exoskeleton under proportional EMG control. We assessed effort by measuring EMG activations and biological knee torque generation on the affected and unaffected sides. We assessed symmetry by measuring ground reaction forces and computing the center of pressure and the center of mass displacement. The results of this case study provide

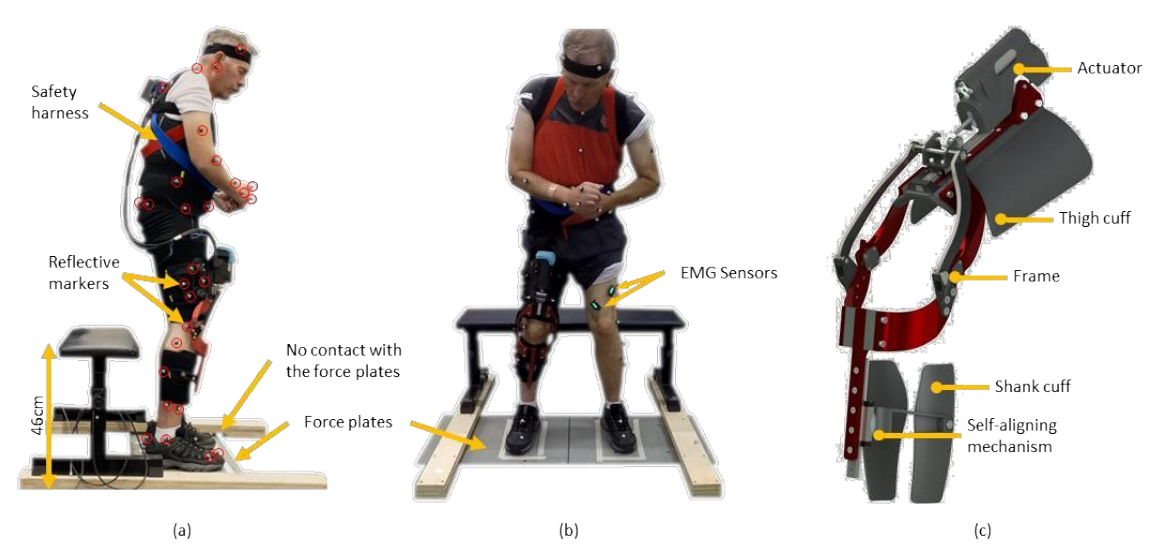


Fig. 1. (a) Side view of the subject during the experiment. Red circles are placed around the reflective markers for motion capture. The subject wore a safety harness that wraps around the subject's upper body and is anchored to a beam through an auto-locking device. The safety rope is not shown in the figure. Boxes were taped to keep subject's feet position consistent throughout the testing. (b) Frontal view of the subject during the experiment. EMG sensors were placed on select subject's lower-limb muscles. Suspended wooden platforms were used to prevent the bench from making contact with the force plates. The experimenters ensured that there is no contact between the wooden platforms and the force plates. (c) CAD model of the Utah ExoKnee (straps are not shown).

information necessary to design future clinical studies with adequate statistical power.

### II. METHODS

#### A. Subject Information

One subject with hemiparesis was recruited for this case study (62 years old, 82 kg, 173 cm, 27 years post-stroke, FAC score: 4). The Institutional Review Board at the University of Utah approved the study protocol. The subject provided informed consent to participate in the study. The subject also provided written consent for the publication of their photos and videos.

# B. Experimental Protocol and Data Analysis

The experiment was performed in a motion capture lab using a 12-camera Vicon system (Vicon Motion Systems Ltd; Oxford, UK) and two AMTI floor force plates (Advanced Mechanical Technology, Inc; Watertown, MA). The subject wore a safety harness connected to overhead support to prevent falls. The subject wore tight-fitting clothes with reflective markers placed on anatomical bony landmarks. We used a modified Plug-in-Gait model [18] with redundant markers placed on the subject's pelvis, legs, and feet for more reliable tracking. We measured muscle activations using two 4-channel EMG sensors (Delsys Trigno Quattro, Research+ System, Delsys Incorporated; Natick MA). The EMG electrodes were placed on the muscle bellies of the Vastus Medialis and Vastus Lateralis muscles on both the affected and unaffected leg because these muscles provide most of the knee extension torque. The subject wore an additional surface EMG electrode (Ottobock) placed on the Vastus Medialis of the affected leg. Marker trajectories were sampled at 200 Hz, and the ground reaction forces from the force plates were sampled at 2000 Hz. All data were synchronized together from the motion capture system to the knee exoskeleton using a myRIO-1900 (National Instruments, USA).

First, we performed a static calibration for the subject-specific motion capture model. For this static calibration, the subject stood still for five seconds with legs shoulder-width apart and arms in front with their elbows slightly bent. Then, we performed a functional knee joint calibration where the subject performed two sit-to-stand repetitions generating a rotation at the knee joint. The functional joint center calibration locates the centers of rotation for the knee joints using the Symmetric Center of Rotation Estimation (SCoRE) and Symmetrical Axis of Rotation Analysis (SARA) [16][17].

After the calibration trials, we performed the acquisition protocol, which consisted of the subject performing sit-tostand transitions on a standard height bench (46 cm) without an arm and backrest. The subject was instructed to keep their feet at shoulder width and fold their arms for each sit-to-stand transition. Also, the subject was asked to stand up at their selfselected pace and pause for three seconds between sitting and standing. First, the subject performed two sets of five sit-tostand transitions without using the exoskeleton (i.e., No Exo condition). Then, the subject rested for 30 minutes. After resting, the subject donned the powered knee exoskeleton and repeated the static and joint center calibrations. The sit-tostand trials were repeated in five sets of five, allowing the participant to acclimatize to the exoskeleton assistance. The final five sit-to-stands from the captures with and without the exoskeleton were used for data analysis (i.e., Exo condition).

### C. Powered Knee Exoskeleton

For this study, we used a powered knee exoskeleton, namely Utah ExoKnee, which has been successfully tested with healthy subjects [17] (Fig. 1(c)). The Utah ExoKnee uses a high-power series-elastic actuator (Orion P-170, Apptronik, USA) in combination with a four-bar linkage. The frame of the exoskeleton connects to the wearer's thigh through a plastic cuff, the inner surface of which is lined with Velcro. The subject wears a strap around their waist and thigh for additional support. The shell is tightened around the thigh

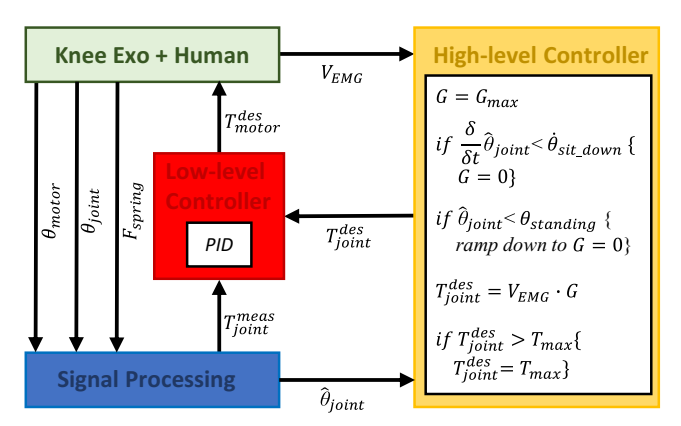


Fig. 2. Block diagram of the control and signal processing systems. All variables are defined and described in section *D. Proportional EMG Control*. At the high-level, a controller based on a proportional EMG controller that defines the desired knee torque. At the low-level, a closed-loop torque controller defines the desired motor current that is then imposed using a motor driver. Raw signals are processed in the embedded electronics.

using BOA® straps with magnetic buckles. The shank segment uses a C-shaped frame with a suspended wrap. The Utah ExoKnee features a compact and lightweight selfaligning mechanism with three passive degrees of freedom. The self-aligning mechanism has been shown to improve subject comfort and task performance during sit-to-stand transitions [13]. The weight of the exoskeleton without the electronics pack is 2.5 kg.

The Utah ExoKnee is controlled using an onboard computer (myRIO-1900, National Instruments, USA). Sensor reading and filtering run at 500 Hz, while the low-level control loop runs at 1 kHz. The onboard computer communicates with the motor current servo controller (ESCON 70/10, Maxon Motor, Switzerland). An external laptop runs a custom graphical user interface (GUI) for data monitoring and parameter-selection purposes and communicates via Wi-Fi with the onboard computer. The GUI is used to change the control parameters and start/stop data saving. The weight of the electronics pack, including the battery and protective covers, is 1.1 kg.

# D. Proportional EMG Control

For the proposed sit-to-stand experiments, we used a proportional EMG controller [21]. Proportional EMG control has been successfully used in upper [22] and lower limb [21] exoskeletons and prostheses. Our assistive controller uses the EMG activation of the vastus medialis on the affected side to define the desired extension knee torque during sit-to-stand transitions (Fig. 2). Specifically, when the subject stands up, the EMG signal is multiplied by a proportional gain (G = $G_{max}$ ) to define the desired knee extension torque. The desired torque saturates at the maximum value  $(T_{max})$  which was set to 40Nm based on subject's feedback. Moreover, after the knee joint angle exceeds a set threshold ( $\theta_{standing}$ ) the proportional gain (G) ramps down to zero. The controller parameters ( $T_{max}$ ,  $G_{max}$ ,  $\theta_{standing}$ ,  $\dot{\theta}_{sitdown}$ ) are adjusted by the experimenter through a GUI. For the goal of this experiment, only the sit-to-stand transitions were assisted. The controller automatically switches to a transparent mode (i.e., zero-torque mode) when the subject performs a stand-tosit transition and the knee velocity exceeds a specified knee velocity threshold  $(\frac{\delta}{\delta t} \hat{\theta}_{joint} < \dot{\theta}_{sitdown})$ .

At the low-level, the assistive controller uses a closed-loop PID regulator to accurately track the desired knee torque defined by the high-level controller ( $T_{joint}^{des}$ ). First, the desired knee torque is converted into desired motor torque ( $T_{motor}^{des}$ ) using the four-bar transmission ratio and the ballscrew and belt transmission ratio. Finally, the desired motor torque is fed to the PID controller and the motor driver.

## E. Data Processing

Experimental data were analyzed with Vicon Nexus 2 (Vicon Motion Systems, Ltd., Oxford, UK), Visual 3D (C-Motion, Maryland, USA), and MATLAB (The MathWorks, Inc. Massachusetts, USA). Core processing operations to automate offline reconstruction, marker labeling, and kinematic fitting were performed in Nexus to produce 3D trajectories from the raw marker data. Once the markers were labeled, their trajectories were processed using fill gap operations, and calibration of joint positions using SCoRE and SARA were performed on the static model and processed dynamic trials.

After data processing operations were performed offline in Nexus, the marker trajectories, force plate analog data, and EMG data were imported into Visual 3D software. A low-

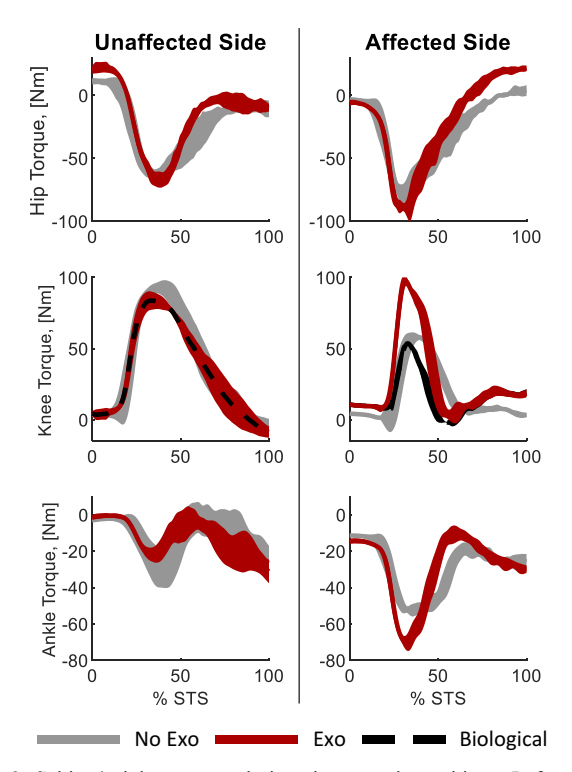


Fig. 3. Subject's joint torques during sit-to-stand transitions. Left column represents subjects unaffected side, the right column represents the subject's affected side. Hip, knee, and ankle torques are shown. The *No Exo* condition is shown in grey, and the *Exo* condition is shown in red. The black dashed line represents biological knee torque. The lines represent data averaged across multiple repetitions. Hip: positive values represent flexion. Knee: positive values represent extension. The knee torque of the affected side during the Exo condition includes both biological and assistive torque (solid line). Ankle: positive values represent dorsiflexion. The shaded regions represent one standard deviation above and below the average values.

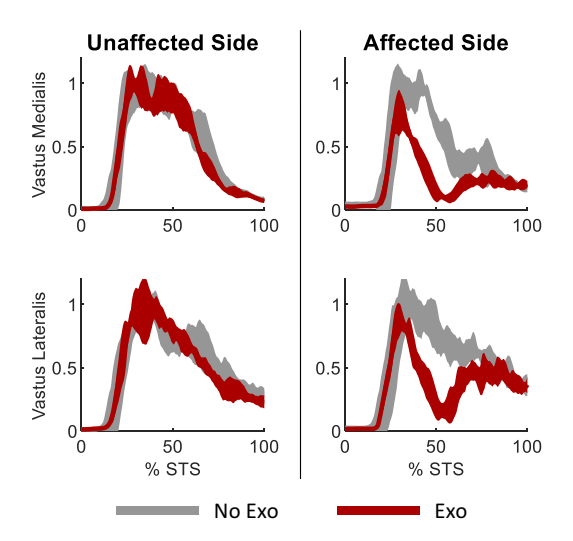


Fig. 4. Subject's EMG muscle readings during sit-to-stand transitions. Left column represents subjects unaffected side, while the right column represents the subject's affected side. Vastus Medialis and Vastus Lateralis muscle EMG data are shown. The *No Exo* condition is shown in grey, and the *Exo* condition is shown in red. The solid lines represent data averaged across multiple repetitions. The shaded regions represent one standard deviation above and below the average values.

pass fourth-order Butterworth filter was applied to both the marker trajectories and analog force plate data with a cutoff frequency of 6 Hz and 15 Hz, respectively. Cutoff frequencies were determined using residual analysis and visual inspection [23]. Kinematics and kinetics were computed using the joint centers of rotation for the ankle, knee, and hip for both legs using Visual 3D. The V3D Composite Pelvis was used for all kinematic and kinetic analyses [24]. All inverse dynamic calculations were computed in Visual 3D and imported into MATLAB.

All data imported into MATLAB were resampled to 2,000 Hz to match the frequency of the force plate data. The raw EMG signals were bandpass filtered with cutoff frequencies of 20 and 450 Hz. The rectified EMG signal was then low pass filtered at 2 Hz. The kinetics, kinematics, ground reaction force (GRF), and EMG data were resampled to 1,000 samples and segmented using thresholds for knee joint position and velocity to only include the standing up motion. Similar to previous exoskeleton studies [25], we calculated the biological torques generated by the subject by assuming that the exoskeleton assistive torque is perfectly transferred to

the subject's leg. Thus, we subtracted the assistive torque measured by the exoskeleton from the subject's knee torque calculated through inverse dynamics to obtain the biological knee torque.

The acquired data were averaged across the repetitions after time normalization based on sit-to-stand transition time (Fig. 3) for both *No Exo* (grey) and *Exo* (red) conditions. The EMG data were averaged across the repetitions after time normalization based on sit-to-stand transition time (Fig. 4) for both *No Exo* (grey) and *Exo* (red) conditions. Additionally, time-space integrated EMG values were calculated to estimate the duration and level of muscle activation. Medial-lateral balance is a common metric for quantifying subject sit-to-stand performance [26]. In this study, the subject's balance was quantified using a Degree of Asymmetry (DOA) measure used previously with amputees [27]. The DOA is calculated using the ground reaction force (GRF) data (1).

$$DOA = \frac{GRF_{sound \ side} - GRF_{impaired \ side}}{GRF_{sound \ side} + GRF_{impaired \ side}} \cdot 100\% \tag{1}$$

A positive value of the DOA indicates greater asymmetry towards the subject's unaffected side, while a negative value of the DOA indicates greater asymmetry towards the affected side (Fig. 5 (a)). A value of zero indicates perfect balance. The DOA was calculated at the point of the largest value of GRF.

# III. RESULTS

# A. Joint Torques

The peak of the hip joint torque increased by 8.95% (unaffected side) and 10.7% (affected side) during the *Exo* condition compared to the *No Exo* condition. In contrast, the peak of the biological knee joint torque decreased by 6.24% (unaffected side) and 11.9% (affected side) during the *Exo* condition compared to the *No Exo* condition. Finally, the peak of the ankle plantarflexion torque on the affected side was 25.6% higher during the *Exo* condition compared to the *No Exo* condition.

## B. Muscle EMG

The peak values of the EMG signals were similar for both Vastus Medialis and Vastus Lateralis on the subject's unaffected side. On the affected side, the peak values of Vastus Medialis and Vastus Lateralis were lower by 29.3% and 21.9%, respectively, during the *Exo* condition compared

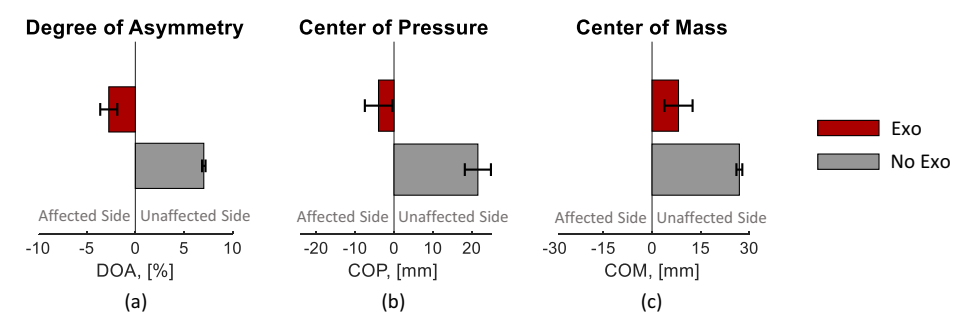


Fig. 5. Degree of Asymmetry (a), the location of the Center of Pressure (b), and the location of the Center of Mass (c) during the sit-to-stand transitions. All metrics were calculated at the point of the maximum ground reaction force. The COP and the COM were calculated with respect to the center position between the feet that was calculated using the force plate data during every sit-to-stand transition. The average values are shown with the error bars representing the standard error. The *No Exo* condition is shown in grey, and the *Exo* condition is shown in red.

to the *No Exo* condition. On the unaffected side, the timeintegrated EMG values of Vastus Medialis and Vastus Lateralis were lower by 10.6% and 9.62%, respectively, during the *Exo* condition compared to the *No Exo* condition. On the affected side, the time-integrated EMG values of Vastus Medialis and Vastus Lateralis were lower by 46.7% and 36.1%, respectively, during the *Exo* condition compared to the *No Exo* condition.

## C. Balance During the Sit-to-Stand Transitions

The DOA during the No Exo condition was 7.04±0.18%. During the Exo condition, the DOA was  $-2.73\pm0.88\%$ . Force plate data were used to calculate the subject's center of pressure (COP) during the sit-to-stand transitions (Fig. 5 (b)). The COP was calculated at the point of the largest value of GRF. During the No Exo condition, the COP location was 21.6±3.36 mm. The location of the COP was -3.98±3.50 mm during the *Exo* condition. Similar to the location of the COP, the Center of Mass (COM) of the subject during the sit-tostand transitions was calculated from the segment masses and locations and then projected onto the ground to remove the vertical component and place it in the same coordinate system as the COP (Fig. 5 (c)). The COM was calculated at the point of the largest value of GRF. When in No Exo condition, the location of the COM was 27.0±0.91 mm. The location of the COM was 8.10±4.34 mm during the *Exo* condition.

### IV. DISCUSSION

# A. Motivation

When standing up, the overexertion of the unaffected side results in greater fatigue in stroke survivors than in healthy individuals [8]. The overexertion results in movement asymmetry and unnatural postural sway, which have been linked to an increased risk of falling [9]. This case study shows that a unilateral powered knee exoskeleton helps reduce muscle effort and improve symmetry during sit-to-stand transitions. By reducing effort and improving balance, a powered knee exoskeleton may improve the mobility and quality of life of many stroke survivors.

# B. Human Experiments and Results

Measuring muscle activations with electromyography provides a reliable way to assess effort. Our results show that the peaks of the EMG signals recorded from the affected quadriceps are visibly lower (29.3% and 21.9%) with the exoskeleton than without the exoskeleton (affected side, Fig. 4). Most important, the integral of the EMG signals for both the Vastus Medialis and the Vastus Lateralis decreases by up to 46.7% with the exoskeleton assistance compared to not wearing the exoskeleton. Therefore, our results suggest that the exoskeleton assistance decreased both the maximum muscle effort and the cumulative (i.e., integral) muscle effort. However, the reduction in the cumulative effort is much greater than the reduction in the peak effort. Interestingly, there is no noticeable reduction in muscle effort for the unaffected leg (Fig. 4). Thus, our result suggests that the knee exoskeleton assistance has a substantial effect on muscle effort on the affected side but only a minimal effect on the unaffected side.

Inverse dynamics provides a reliable way to assess the biological knee torque generated by the affected and unaffected leg. The inverse dynamics results show a slight reduction of the peak biological torque of the knee on both the affected and unaffected leg (Fig. 3). Moreover, with the exoskeleton, there is a substantial reduction of the biological knee torque on the affected leg as the sit-to-stand movement progresses, likely resulting from the continued assistance provided by the knee exoskeleton. Interestingly, the sum of the biological and assistive torque (i.e., ~100 Nm, Fig. 3) on the affected side is much greater with the exoskeleton than without the exoskeleton. Moreover, the total knee torque profiles of the affected side and unaffected side are more similar with the exoskeleton than without the exoskeleton. Interestingly, the peak torque at the hip and ankle joint were slightly higher with the exoskeleton than without the exoskeleton. However, after achieving their peaks, both the hip and ankle torque are visibly lower with the exoskeleton than without the exoskeleton. Thus, our result suggests that the exoskeleton assistance reduced the knee biological knee torque on both the affected and unaffected sides while reducing the asymmetry in total knee torque between the two sides.

Balance during sit-to-stand transitions can be assessed in different ways. Our results show that the degree of asymmetry decreased from 7.04% without the exoskeleton to -2.73% with the exoskeleton, suggesting a shift from the unaffected side bias to the affected side bias (Fig. 5 (a)). Similarly, the average medial-lateral location of the center of pressure changed from 21.6 mm without the exoskeleton to -3.98 mm (Fig. 5 (b)). These results also show that the exoskeleton allows for a more symmetric movement, with a small bias towards the affected side. Finally, the results show a reduction in the average location of the center of mass from 27.0 mm without the exoskeleton to 8.10 mm with the exoskeleton (Fig. 5(c)). Thus, the center of mass was more centered with the exoskeleton than without the exoskeleton. Therefore, all three measures of balance suggest that the assistance provided by the exoskeleton can provide considerable improvements during sit-to-stand transitions.

### C. Limitations and Future Work

Despite the encouraging outcomes of this case study, there are some limitations to consider. Like in all case studies, the results of this experiment may not generalize to a broader population. This limitation is particularly important given the wide variability observed in individuals with hemiparesis. The level of assistance provided by the exoskeleton was based on the subjective feedback received from the study participant subject as well as the results of previous studies with healthy subjects.

Future work will focus on testing the protocol with a larger number of hemiparetic subjects to confirm the results statistically. It is also likely that the assistance provided by the exoskeleton was not optimal. In this study, we rely on subjective feedback for tuning. This approach has previously been shown successful [28]. However, future studies should investigate the effect of different assistance levels, for example, by using different gains for the proportional EMG

controller. Alternatively, future studies should use the humanin-the-loop [29] approach to find the optimal gain of the proportional controller. A possible future direction is also to use the exoskeleton during other ambulatory activities such as walking, stairs ambulation, and ramped surfaces.

#### V. CONCLUSION

Muscle weakness and lack of control on one side of the body severely affect the ability of stroke survivors to perform activities of daily living. Currently, the effects of using powered exoskeletons on stroke survivors are unknown. Our results show that when assisted by a powered exoskeleton, a hemiparetic subject exerts a lower level of joint torque as well as lower muscle activation. Additionally, using the exoskeleton helped improve the subject's balance when standing up based on DOA, COP, and COM. Future work will focus on expanding the experiments to a larger number of hemiparetic subjects and investigating different levels of assistance. Finally, future studies will include testing other ambulatory activities such as walking and stairs ambulation.

#### ACKNOWLEDGMENT

The authors would like to thank Grace Hunt, Dr. Steven Edgley, and the members of the Bionic Engineering Lab for their help with testing and subject recruitment.

#### REFERENCES

- E. J. Benjamin et al., "Heart Disease and Stroke Statistics-2019 Update: A Report From the American Heart Association," Circulation, 2019, doi: 10.1161/CIR.0000000000000659.
- [2] I. Jonkers, S. Delp, and C. Patten, "Capacity to increase walking speed is limited by impaired hip and ankle power generation in lower functioning persons post-stroke," *Gait and Posture*, 2009, doi: 10.1016/j.gaitpost.2008.07.010.
- [3] M. M. Rybar *et al.*, "The stroke-related effects of hip flexion fatigue on over ground walking," *Gait and Posture*, 2014, doi: 10.1016/j.gaitpost.2014.01.012.
- [4] D. Mozaffarian et al., "Heart Disease and Stroke Statistics—2016 Update," Circulation, vol. 133, no. 4, pp. e38–e360, 2016, doi: 10.1161/CIR.0000000000000350.
- [5] P.-T. Cheng, S.-H. Wu, M.-Y. Liaw, A. M. K. Wong, and F.-T. Tang, "Symmetrical body-weight distribution training in stroke patients and its effect on fall prevention," *Archives of Physical Medicine and Rehabilitation*, vol. 82, no. 12, pp. 1650–1654, Dec. 2001, doi: 10.1053/apmr.2001.26256.
- [6] M. Y. Lee, M. K. Wong, F. T. Tang, P. T. Cheng, and P. S. Lin, "Comparison of Balance Responses and Motor Patterns During Sit-To-Stand Task with Functional Mobility in Stroke Patients," *American Journal of Physical Medicine & Rehabilitation*, vol. 76, no. 5, pp. 401–410, Sep. 1997, doi: 10.1097/00002060-199709000-00011.
- [7] G. Roy, S. Nadeau, D. Gravel, F. Piotte, F. Malouin, and B. J. McFadyen, "Side difference in the hip and knee joint moments during sit-to-stand and stand-to-sit tasks in individuals with hemiparesis," *Clinical Biomechanics*, vol. 22, no. 7, pp. 795–804, Aug. 2007, doi: 10.1016/j.clinbiomech.2007.03.007.
- [8] M. M. Rybar et al., "The stroke-related effects of hip flexion fatigue on over ground walking," Gait and Posture, vol. 39, no. 4, pp. 1103– 1108, 2014, doi: 10.1016/j.gaitpost.2014.01.012.
- [9] M. Y. Lee, "The sit-to-stand movement in stroke patients and its correlation with falling."
- [10] P. Wretenberg and U. P. Arborelius, "Power and work produced in different leg muscle groups when rising from a chair," *European Journal of Applied Physiology and Occupational Physiology*, vol. 68, no. 5, pp. 413–417, 1994, doi: 10.1007/BF00843738.

- [11] A. J. Young and D. P. Ferris, "State of the art and future directions for lower limb robotic exoskeletons," *IEEE Transactions on Neural Systems and Rehabilitation Engineering*, vol. 25, no. 2, pp. 171–182, Feb. 2017, doi: 10.1109/TNSRE.2016.2521160.
- [12] M. K. Shepherd and E. J. Rouse, "Design and Validation of a Torque-Controllable Knee Exoskeleton for Sit-to-Stand Assistance," IEEE/ASME Transactions on Mechatronics, vol. 22, no. 4, pp. 1695–1704, 2017, doi: 10.1109/TMECH.2017.2704521.
- [13] S. V. Sarkisian, M. K. Ishmael, and T. Lenzi, "Self-Aligning Mechanism Improves Comfort and Performance with a Powered Knee Exoskeleton," *IEEE Transactions on Neural Systems and Rehabilitation Engineering*, vol. 29, pp. 629–640, 2021, doi: 10.1109/TNSRE.2021.3064463.
- [14] H. Zhu, C. Nesler, N. Divekar, V. Peddinti, and R. Gregg, "Design Principles for Compact, Backdrivable Actuation in Partial-Assist Powered Knee Orthoses," *IEEE/ASME Transactions on Mechatronics*, pp. 1–1, 2021, doi: 10.1109/TMECH.2021.3053226.
- [15] G. Choi, D. Lee, I. Kang, and A. J. Young, "Effect of Assistance Timing in Knee Extensor Muscle Activation During Sit-to-Stand Using a Bilateral Robotic Knee Exoskeleton," in 2021 43rd Annual International Conference of the IEEE Engineering in Medicine & Biology Society (EMBC), Nov. 2021, pp. 4879–4882. doi: 10.1109/EMBC46164.2021.9629965.
- [16] X. Liu, Z. Zhou, J. Mai, and Q. Wang, "Real-time mode recognition based assistive torque control of bionic knee exoskeleton for sit-tostand and stand-to-sit transitions," *Robotics and Autonomous Systems*, vol. 119, pp. 209–220, Sep. 2019, doi: 10.1016/j.robot.2019.06.008.
- [17] S. V. Sarkisian, M. K. Ishmael, G. R. Hunt, and T. Lenzi, "Design, Development, and Validation of a Self-Aligning Mechanism for High-Torque Powered Knee Exoskeletons," *IEEE Transactions on Medical Robotics and Bionics*, vol. 2, no. 2, pp. 248–259, 2020, doi: 10.1109/tmrb.2020.2981951.
- [18] S. Hood, M. K. Ishmael, A. Gunnell, K. B. Foreman, and T. Lenzi, "A kinematic and kinetic dataset of 18 above-knee amputees walking at various speeds," *Scientific Data*, vol. 7, no. 1, p. 150, Dec. 2020, doi: 10.1038/s41597-020-0494-7.
- [19] R. M. Ehrig, W. R. Taylor, G. N. Duda, and M. O. Heller, "A survey of formal methods for determining the centre of rotation of ball joints," *Journal of Biomechanics*, vol. 39, no. 15, pp. 2798–2809, 2006, doi: 10.1016/j.jbiomech.2005.10.002.
- [20] W. R. Taylor et al., "Repeatability and reproducibility of OSSCA, a functional approach for assessing the kinematics of the lower limb," *Gait and Posture*, vol. 32, no. 2, pp. 231–236, Jun. 2010, doi: 10.1016/j.gaitpost.2010.05.005.
- [21] C. R. Kinnaird and D. P. Ferris, "Medial gastrocnemius myoelectric control of a robotic ankle exoskeleton," in *IEEE Transactions on Neural Systems and Rehabilitation Engineering*, Feb. 2009, vol. 17, no. 1, pp. 31–37. doi: 10.1109/TNSRE.2008.2008285.
- [22] T. Lenzi, S. M. M. de Rossi, N. Vitiello, and M. C. Carrozza, "Intention-based EMG control for powered exoskeletons," *IEEE Transactions on Biomedical Engineering*, vol. 59, no. 8, pp. 2180–2190, 2012, doi: 10.1109/TBME.2012.2198821.
- [23] D. Winter, Biomechanics and motor control of human gait: normal, elderly and pathological, 2nd ed. Waterloo Biomechanics Press, 1991
- [24] C-Motion WIKI Documentation, "V3D Composite Pelvis," Jul. 17, 2019.
- [25] D. J. Farris and G. S. Sawicki, "Linking the mechanics and energetics of hopping with elastic ankle exoskeletons," *J Appl Physiol*, vol. 113, pp. 1862–1872, 2012, doi: 10.1152/japplphysiol.00802.2012.-The.
- [26] M. Y. Lee, "The sit-to-stand movement in stroke patients and its correlation with falling."
- [27] M. J. Highsmith *et al.*, "Kinetic asymmetry in transfemoral amputees while performing sit to stand and stand to sit movements," *Gait and Posture*, vol. 34, no. 1, pp. 86–91, May 2011, doi: 10.1016/j.gaitpost.2011.03.018.
- [28] M. K. Ishmael, D. Archangeli, and T. Lenzi, "Powered hip exoskeleton improves walking economy in individuals with aboveknee amputation," *Nature Medicine*, vol. 27, no. 10, pp. 1783–1788, Oct. 2021, doi: 10.1038/s41591-021-01515-2.
- [29] J. Zhang et al., "Human-in-the-loop optimization of exoskeleton assistance during walking."